

Keywords: classification, remote sensing, soil adjusted vegetation index, normalized difference vegetation index, vegetation

Anusha NALLAPAREDDY [0000-0002-2115-5998]*

DETECTION AND CLASSIFICATION OF VEGETATION AREAS FROM RED AND NEAR INFRARED BANDS OF LANDSAT-8 OPTICAL SATELLITE IMAGE

Abstract

Detection and classification of vegetation is a crucial technical task in the management of natural resources since vegetation serves as a foundation for all living things and has a significant impact on climate change such as impacting terrestrial carbon dioxide (CO₂). Traditional approaches for acquiring vegetation covers such as field surveys, map interpretation, collateral and data analysis are ineffective as they are time consuming and expensive. In this paper vegetation regions are automatically detected by applying simple but effective vegetation indices Normalized Difference Vegetation Index (NDVI) and Soil Adjusted Vegetation Index (SAVI) on red(R) and near infrared (NIR) bands of Landsat-8 satellite image. Remote sensing technology makes it possible to analyze vegetation cover across wide areas in a cost-effective manner. Using remotely sensed images, the mapping of vegetation requires a number of factors, techniques, and methodologies. The rapid improvement of remote sensing technologies broadens possibilities for image sources making remotely sensed images more accessible. The dataset used in this paper is the R and NIR bands of Level-1 Tier 1 Landsat-8 optical remote sensing image acquired on 6th September 2013, is processed and made available to users on 2nd May 2017. The pre-processing involving sub-setting operation is performed using the ERDAS Imagine tool on R and NIR bands of Landsat-8 image. The NDVI and SAVI are utilized to extract vegetation features automatically by using python language. Finally by establishing a threshold, vegetation cover of the research area is detected and then classified.

1. INTRODUCTION

Vegetation is a huge and complex subject spanning a wide range of plant life as shown in Fig. 1. There are many different classification systems for vegetation, each with its own set of criteria (Persson, Ulander & Soja, 2018, Ruiz et al., 2021). It has become a critical technological challenge for managing natural resources, and vegetation plays a significant role in global climate change such as impacting terrestrial CO₂ (Yu, Xie & Sha, 2008).

* Vidya Jyothi Institute of Technology, Department of Computer Science and Engineering, India, anusha.nallapareddy@gmail.com

Vegetation extraction involves understating the Color, texture, tone, pattern, and association information in the satellite images (Gandhi, Parthiban & Christy, 2015). To do this, various methods are developed. These are often categorized into supervised and unsupervised methods (Porikli et al., 2017). Vegetation detection includes image pre-processing and image classification.

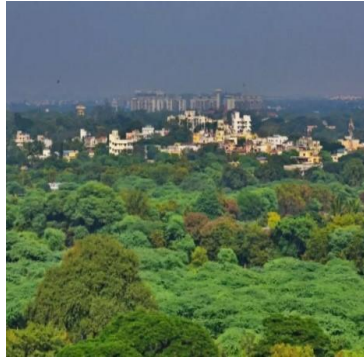


Fig. 1. Vegetation cover

1.1. Image Pre-processing

Satellite imaging is used for a variety of purposes including assessing and monitoring the state of the earth's surface, disaster management and the study of natural disaster images, Land Use Land Cover (LULC) mapping, and LULC-based mapping modifications (Dalponte et al., 2020).

The goal of pre-processing operations is enhancing images (Bouhennache, Bouden & Taleb, 2014). To eliminate noise and improve the interpretability of image data, satellite images must be pre-processed before vegetation extraction (Yu, Xie & Sha, 2008). Pre-processing of remote sensing data includes geometric correction, atmospheric correction, and topographic correction (Jing et al., 2009). To account for surface reflectivity, all photos are atmospherically corrected (Fatihaa et al., 2013). The LEDAPS system is used to process the Landsat 5 and 7 images. Landsat-8 satellite images are processed by the Landsat-8 Surface Reflectance (L8SR) system (Schmidt et al., 2013).

Prior to vegetation extraction, satellite image preparation is required to eliminate noise and improve the interpretability of satellite image data. This is especially true when a temporal series of images is employed or when a large area is covered by multiple photographs, because it is critical to make these images spatially and spectrally consistent. Although image pre-processing varies depending on the sensor used, it usually entails a series of steps including radiometric correction, geometric correction, image enhancement, and masking (for clouds, water etc.) (Yu, Xie & Sha, 2008).

The practice of fixing radiometric defects or distortions in images to enhance the accuracy of brightness values is known as radiometric correction of remote sensing data. Seasonal phenology, ground conditions, and atmospheric variables significantly influence multi-temporal spectral response variability. To identify noise, radiometric correction is essential when the spectral signals are insufficiently strong to exclude the impacts of these intricate components (Chen, Giri & Vogelmann, 2016).

Geometric correction's main purpose is to remove geometric distortions from affected images. It is done by creating a link between the image coordinate system and the geographic coordinate system utilizing the sensor's calibration data, position and altitude readings, and ground control points. As a result, geometric corrections require choosing a map projection system and co-registering satellite image data with other data that serves as a calibration reference. It is done by using the sensor's calibration data, position and altitude readings, and ground control points to create a link between the image coordinate system and the geographic coordinate system (Jing et al., 2009).

The USGS Earth Resources Observation and Science Centre provides Landsat-8 satellite products that are/can be radiometrically corrected, atmospherically corrected, terrain corrected (Li et al., 2017).

1.2. Vegetation Detection

Among vegetation indices, NDVI is one of the most widely used techniques. It is the best indicator for crop condition and spatial distribution. A combination of red and near-infrared bands are used to determine NDVI (Jing et al., 2009).

NDVI is a good indicator for reflecting dynamic changes in vegetation groupings. Individual vegetation groups can be defined based on their distinct phenology or dynamic NDVI signals (Yu, Xie & Sha, 2008).

Huete proposed a SAVI index with an adjustment parameter, indicating L that characterizes the ground and its rate of vegetation cover. The isolines vegetation is not aligned to the right-hand side of the grounds, but they cut this one in a place shown by Huete based on the density of vegetation cover. For a heavy density of vegetation, the parameter L is set to 0.25, while for a very low density of vegetation, it is set to 1. The value is equivalent to 0.5 at intermediate densities (Fatihaa et al., 2013).

1.3. Image Classification

The technique of deriving unique classifications or themes (e.g., land use categories, vegetation species) from raw remotely sensed satellite data is known as image classification. Obviously, image pre-processing is included in this definition. The technique that follows image pre-processing is simply referred to as image classification. Traditional and improved methods are two techniques for extracting vegetation from pre-processed images (Yu, Xie & Sha, 2008).

Landsat-8 data is compared to older Landsat data, the surface reflectance of the six optical bands is measured, and two VIs are created (NDVI and EVI) and land use inventory map with labelled training samples and simple linear trend is used to detect changes and classify them as abrupt or gradual changes (Zhu et al., 2016).

Landsat images (He et al., 2020; Dutta, Rahman & Kundu, 2015) are used and sub pixel analysis is performed because each pixel may not belong to a single class (pure pixel). For dimensionality, Principal Component Analysis is utilized. Reduction and Linear Spectral unmixing is used for classification and simple image differencing is used to detect change (Dutta, Rahman & Kundu, 2015).

The CCDC algorithm is used to detect and classify land cover changes. Correction of the BRDF impact for each Landsat image in order to provide a more uniform LTS, with the hope of improving both change detection and classification. The Support Vector Machine (SVM) is a nonlinear classification approach that is used to classify images and forecast disease (He et al., 2020).

The spectra of the same type of surface object are approximately linearly scaled replicas of one another due to atmospheric and topographic influences. Spectral angle classifiers (SAC) both supervised and unsupervised are employed to account for this. The distances between pairs of signatures for categorization, as well as the classification of biotic communities and land cover, are successfully determined using these SACs (Yu, Xie & Sha, 2008).

2. METHODOLOGY

2.1. Study Area and Dataset Used

The study is conducted in districts of Uttar Pradesh with latitude 24°57'12.07"–27°01'54.86" North and longitude 82°14'49.38"–84°27'49.00" East, as this area has a large cover of vegetation. Fig. 2 shows a Google Earth Engine view of the research area.

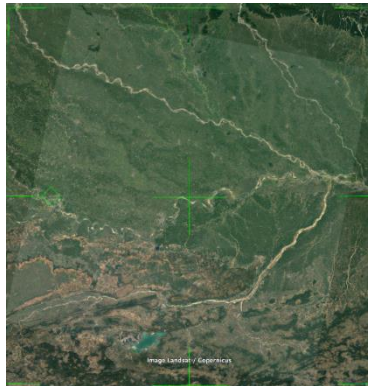


Fig. 1. View of study area (Credits: Google Earth Engine platform)

In this research, the satellite image collected by Landsat-8 is used. The USGS and NASA collaborate on the Landsat series to observe the earth. The Landsat-8 satellite image has a resolution of 30 meters. R and NIR bands are used to classify healthy vegetation. R and NIR bands have wavelengths of 0.64–0.67 and 0.85–0.88 micrometers respectively (Roy et al., 2014).

A Level-1 Tier 1 Landsat-8 satellite image is collected from the website USGS Earth Explorer, which provides free access to satellite images of different satellites. The satellite image collected contains information captured by both Landsat-8's operational land imager (OLI) and thermal infrared sensor (TIRS) sensors of 142 Worldwide Reference System (WRS) path and 042 WRS row. The image is Precision and Terrain Corrected (L1TP) (Landsat Missions, n.d.) and was acquired on 6th September 2013, is processed and made available to users on 2nd May 2017.

2.2. Research Methodology

Landsat-8 satellite image acquired on 6th September 2013 and made available to users on 2nd May 2017 is considered as the input. R and NIR bands of this image are used in this study to classify healthy vegetation. As the satellite image acquired is too large to be processed, sub-setting is performed on R and NIR bands of the input image to obtain an Area of Interest (AOI). The pre-processing step is carried out in ERDAS Imagine tool (Asokan et al., 2020; Abburu & Golla, 2015).

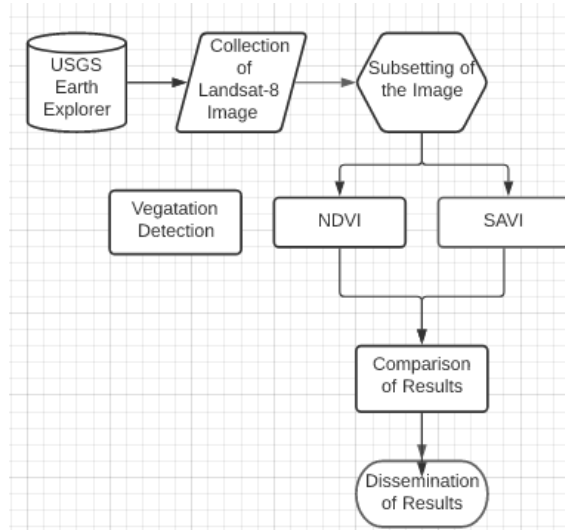


Fig. 2. Flowchart of the applied methodology

To extract the vegetation features (Ahmad et al., 2020; Langendoen et al., 2020) automatically, vegetation indices like NDVI, and SAVI are utilized (Sowmya, Deepa & Venugopal, 2017). Fig. 3 depicts the flow diagram of the applied methodology in this work. The vegetation features for the input satellite image are classified by applying threshold values for the computed vegetation indices (Xue & Su, 2017).

2.2.1. NDVI

NDVI is calculated as a ratio between R and NIR bands (Yu, Xie & Sha, 2008) using the Equation (1).

$$NDVI = \frac{NIR-R}{NIR+R} \quad (1)$$

In the image collected by the Landsat-8 satellite, band 5 corresponds to NIR band and band 4 corresponds to R band (Omar & Kawamukai, 2021; Rhyma et al., 2019). By substituting band 5 and band 4 in place of NIR and R bands respectively in Equation (1), NDVI for Landsat-8 image is calculated using the Equation (2).

$$NDVI = \frac{\text{band 5}-\text{band 4}}{\text{band 5}+\text{band 4}} \quad (2)$$

2.2.2. SAVI

SAVI is calculated as a ratio of the R and NIR bands with a soil brightness correction factor (L) (Rhyma et al., 2019) as given in Equation (3).

$$\text{SAVI} = (\text{NIR} - \text{R}) / (\text{NIR} + \text{R})(1 + \text{L}) \quad (3)$$

By substituting band 5 and band 4 in place of NIR and R bands respectively in Equation (3) and L with 0.5 (Rhyma et al., 2019), SAVI for Landsat-8 image is calculated using the Equation (4).

$$\text{SAVI} = (\text{band 5} - \text{band 4}) / (\text{band 5} + \text{band 4})(1 + \text{L}) \quad (4)$$

2.3. Technologies Used

The satellite image acquired is in GeoTiff format because it contains georeferencing information embedded in the GeoTiff file. Python 3.6.9 has a Rasterio library which can be used to work with this kind of input images. EarthPy is a python package devoted to working with spatial and remote sensing data. EarthPy has several Python package dependencies including rasterio, geopandas, numpy.

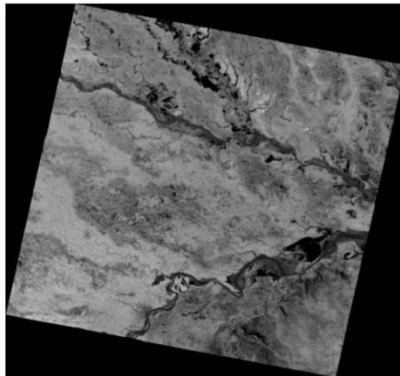


Fig. 3. Subset of the R band of the Landsat-8 satellite image acquired 6th September 2013

The input images are loaded into google drive and mounted on google collab, an online version of Anaconda jupyter. Fig. 4 and Fig. 5 depicts the red and near infrared bands respectively of Landsat-8 satellite acquired on 6th September 2013.

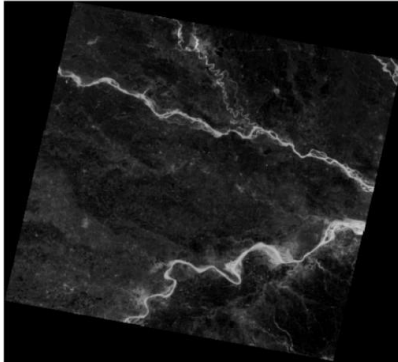


Fig. 4. Subset of the NIR band of the Landsat-8 satellite image acquired on 6th September 2013

3. RESULTS AND DISCUSSIONS

A Landsat-8 satellite image is collected and pre-processing operation such as sub-setting is performed using ERDAS Imagine tool. The spectral bands required for calculating vegetation indices are opened and read using the rasterio library of python to perform the operations on the input image bands. The computed NDVI and SAVI vegetation indices results are then subjective evaluation of the exactness of the vegetation cover is performed with the google Earth Pro view of the Study Area.

3.1. Detection of Vegetation using NDVI

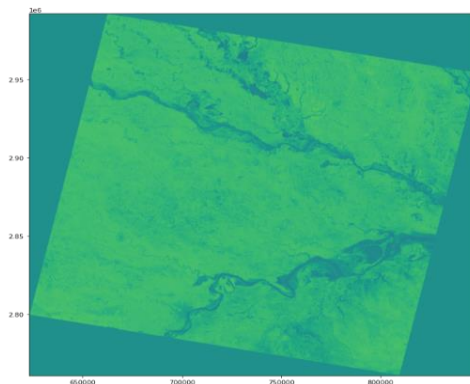


Fig. 5. Results obtained using NDVI

The rasterio library is used to read the bands of input pre-processed Geotiff images containing the AOI. Using the numpy package in python, NDVI is computed and the resultant image is saved in Geotiff image format. Fig. 6 shows the NDVI image obtained after calculation.

3.2. Detection of Vegetation using SAVI

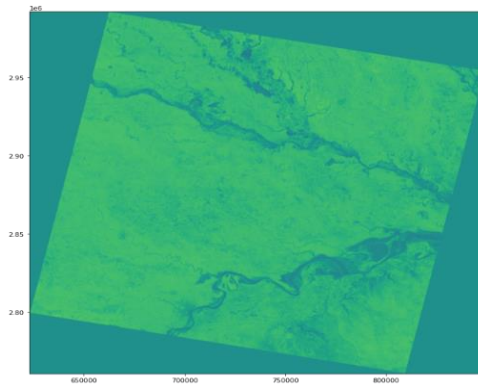


Fig. 6. Results obtained using SAVI

The input bands of pre-processed Geotiff image containing the AOI are read using the rasterio library. SAVI is computed using numpy package in python and the resultant image is saved in Geotiff image format. Fig. 7 shows the SAVI image produced after calculation.

3.3. Comparative Analysis of Results

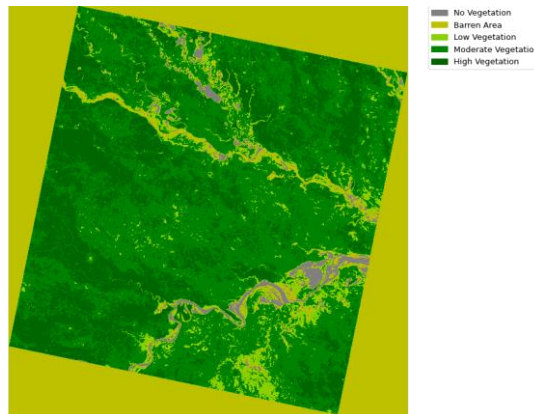


Fig. 7. Classification result of NDVI

Computation of NDVI involved only spectral measurements from the satellite. SAVI, on the other hand, required the estimation of the L parameter, which is difficult to determine. This is due to the fact that not all soils are alike. Due to many factors such as soil moisture, organic content, mechanical composition, ferrous content, etc., various soils have varied reflectance spectra. NDVI less than 0.25 imply that there is no vegetation present, only soil. Water or urban regions have negative values. The thicker (healthier) the vegetation is, the higher the NDVI values (the same is applicable even for SAVI). However, after a value of 0.7, the NDVI begins to rapidly saturate. As a result, SAVI is more suited to dense vegetation since it saturates at a slower pace. When there is more dense vegetation cover, the L parameter must be modified.

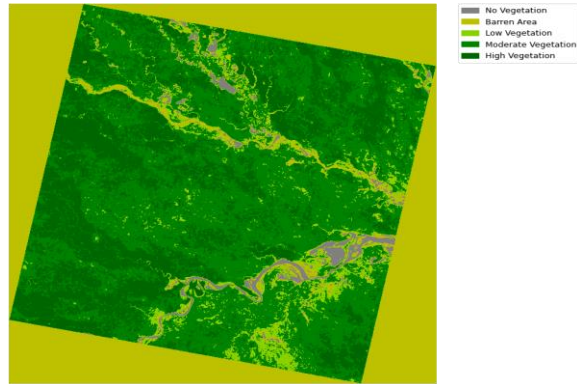
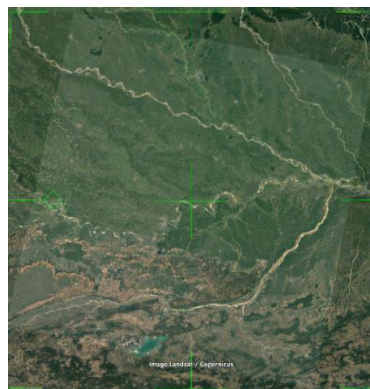


Fig. 8. Classification result of SAVI

Clouds, water, and snow contribute negative values, while rocks and barren soil contribute near-zero values. Barren areas correlate to vegetation indices with very low values (0.25 or below) (empty areas of rocks, sand or snow). Small numbers represent low vegetation levels (between 0.25 and 0.4).



**Fig. 9. Google Earth Pro view of the Study Area
(Credits: Google Earth pro platform)**

Moderate vegetation is represented by values between 0.4 and 0.6, whereas high vegetation is represented by values greater than 0.6. These thresholds are applied on the NDVI and SAVI values and each category of vegetation is represented using different colors as shown in Fig. 8 and Fig. 9. Color grey represents no vegetation, pale yellow (lime) represents bare area, light green represents low vegetation, green represents moderate vegetation, and emerald green represents high vegetation areas (refer Fig. 8 and Fig. 9).

The output of NDVI and SAVI after applying the threshold can be compared by visual inspection with the Google Earth Pro view of the AOI is shown in Fig. 10. The river stream is detected accurately to a greater extent in both NDVI and SAVI. The low vegetation surrounding the river is also identified and when SAVI is used few areas are detected with high vegetation when compared with NDVI.

4. CONCLUSION

This paper applied vegetation indices for extracting vegetative features from remotely sensed R and NIR bands of Landsat-8 satellite image. On the pre-processed R and NIR bands of Landsat-8 images acquired on 6th September 2013, NDVI and SAVI techniques are applied to determine the characterization of the vegetation cover. The perspective on the study area obtained from Google Earth Engine is utilized to do a subjective evaluation of the exactness of the vegetation cover. This study can be utilized by forestry or urban planning departments to estimate the vegetation cover for LULC. This work can be extended by proposing an Artificial Intelligence (AI) based profound learning model to estimate the progressions in vegetation cover. Further change detection in the AOI can be carried out by applying the vegetation detection methods on multi-temporal satellite images.

Funding

This research was not funded by any organization.

Acknowledgments

Authors would like to thank USGS Earth Resources Observation and Science Centre for proving open access to Landsat-8 satellite product also would like to extend thanks to Google Earth pro platform.

Conflicts of Interest

There is no Conflict of Interest.

REFERENCES

- Abburu, S., & Golla, S. B. (2015). An engineering evaluation on the glimpse of satellite image pre-processing utility tools. *Article of Engineering Journal*, 19(5), 1–10. <https://doi.org/10.4186/ej.2015.19.2.129>
- Ahmad, A. M., Minallah, N., Ahmed, N., Ahmad, A. M., & Fazal, N. (2020). Remote sensing based vegetation classification using machine learning algorithms. *2019 International Conference on Advances in the Emerging Computing Technologies (AECT)* (pp. 1–6). IEEE. <https://doi.org/10.1109/AECT47998.2020.9194217>
- Asokan, A., Anitha, J., Ciobanu, M., Gabor, A., Naaji, A., & Hemanth, D. J. (2020). Image processing techniques for analysis of satellite images for historical maps classification – an overview. *Applied Sciences*, 10(12), 1–21. <https://doi.org/10.3390/app10124207>
- Bouhennache, R., Bouden, T., & Taleb, A. A. (2014). Change Detection in Urban Land Cover Using Landsat Images Satellites, A Case Study in Algiers Town. *2014 Tenth International Conference on Signal-Image Technology and Internet-Based Systems* (pp. 622–628). IEEE. <https://doi.org/10.1109/SITIS.2014.57>
- Chen, X., Giri, C., & Vogelmann, J. E. (2016). Land-Cover Change Detection. *Remote Sensing of Land Use and Land Cover* (pp. 152–176). CRC Press. <https://doi.org/10.1201/b11964-14>
- Dalponte, M., Marzini, S., Solano-Correa, Y. T., Tonon, G., Vescovo, L., & Gianelle, D. (2020). Mapping forest wind throws using high spatial resolution multispectral satellite images. *International Journal of Applied Earth Observation Geoinformatics*, 93, 102206. <https://doi.org/10.1016/j.jag.2020.102206>
- Dutta, D., Rahman, A., & Kundu, A. (2015). Growth of Dehradun city: An application of linear spectral unmixing (LSU) technique using multi-temporal landsat satellite data sets. *Remote Sensing Applications: Society and Environment*, 1, 98–111. <https://doi.org/10.1016/j.rsase.2015.07.001>
- Fatihaa, B., Abdelkaderb, A., Latifac, H., & Mohamedd, E. (2013). Spatio temporal analysis of vegetation by vegetation indices from multi-dates satellite images: Application to a semi arid area in ALGERIA. *TerraGreen 13 International Conference 2013 – Advancements in Renewable Energy and Clean Environment, Elsevier, Energy Procedia*, 36, 667–675. <https://doi.org/10.1016/j.egypro.2013.07.077>

- Gandhi, G. M., Parthiban, S., & Christy, N. T. (2015). Ndvi: Vegetation change detection using remote sensing and gis – A case study of Vellore District. *3rd International Conference on Recent Trends in Computing 2015, Elsevier, Procedia Computer Science*, 57, 1199–1210. <https://doi.org/10.1016/j.procs.2015.07.415>
- He, B., Zhang, H., Feng, S., Liu, X., Zhou, Y., & Guan, Y. (2020). Improving land cover change detection and classification with BRDF correction and spatial feature extraction using Landsat Time Series: A case of urbanization in Tianjin, China. *IEEE Journal of Selected Topics in Applied Earth Observation. and Remote Sensing* (vol 13, pp. 4166–4177). IEEE. <https://doi.org/10.1109/JSTARS.2020.3007562>
- Jing, X., Wang, J., Huang, W., Liu, L., & Wang, J. (2009). Study on Forest Vegetation Classification Based on Multitemporal Remote Sensing Images. *Computer and Computing Technologies in Agriculture II, Volume 1. CCTA 2008. IFIP Advances in Information and Communication Technology* (vol 293). Springer. https://doi.org/10.1007/978-1-4419-0209-2_13
- Landsat Missions. (n.d.). Retrieved February 13, 2022 from <https://www.usgs.gov/landsat-missions/landsat-collection-2-level-1-data>
- Langendoen, D., Navarro, G., Willner, W., Keith, D. A., Liu, C., Guo, K., & Meidinger, D. (2020). Perspectives on Terrestrial Biomes: The International Vegetation Classification. *Encyclopedia of the World's Biomes*, 2020, 1–15. <https://doi.org/10.1016/B978-0-12-409548-9.12417-0>
- Li, A., Lei, G., Zhao, W., Nan, X., & Zhang, Z. (2017). Post-earthquake Landslides Mapping from Landsat-8 Data for the 2015 Nepal Earthquake Using a Pixel-Based Change Detection Method. *IEEE Journal of Selected Topics in Applied. Earth Observation and Remote Sensing*, 10, 1758–1768. <https://doi.org/10.1109/JSTARS.2017.2661802>
- Omar, M. S., & Kawamukai, H. (2021). Prediction of NDVI using the Holt-Winters model in high and low vegetation regions: A case study of East Africa. *Scientific African*, 14, e01020. <https://doi.org/10.1007/s40808-018-0431-3>
- Persson, H. J., Ulander, L. M. H., & Soja, M. J. (2018). Modeling and Detection of Deforestation and Forest Growth in Multitemporal TanDEM-X Data. *IEEE Journal of Selected Topic in Applied Earth Observation and Remote sensing*, 11, 3548–3563. <https://doi.org/10.1109/JSTARS.2018.2851030>
- Porikli, F., Bennamoun, M., Khan, S. H., & He, X. (2017). Forest change detection in incomplete satellite images with deep neural networks. *IEEE Transactions on Geoscience and Remote sensing*, 52, 5407–5423. <https://doi.org/10.1109/TGRS.2017.2707528>
- Rhyma, P. P., Norizah, K., Hamdan, O., Faridah-Hanum, I., & Zulfa, A. W. (2019). Integration of normalised different vegetation index and Soil-Adjusted Vegetation Index for mangrove vegetation delineation. *Remote Sensing Applications: Society and Environment*, 17, 1–14. <https://doi.org/10.1016/j.rsase.2019.100280>
- Roy, D. P., Wulder, M. A., Loveland, T. R., Woodcock, C. E., Allen, R. G., Anderson, M. C., Helder, D., Irons, J. R., Johnson, D. M., Kennedy, R., Scambos, T. A., Schaaf, C. B., Schott, J. R., Sheng, Y., Vermote, E. F., Belward, A. S., Bindshadler, R., Cohen, W. B., Gao, F., Hipple, J. D., Hostert, P., Huntington, J., Justice, C. O., Kilic, A., Kovalskyy, V., Lee, Z. P., Lyburner, L., Masek, J. G., McCorkel, J., Shuai, Y., Trezza, R., Vogelmann, J., Wynne, R. H., & Zhu, Z. (2014). Landsat-8: Science and product vision for terrestrial global change research. *Remote Sensing of Environment*, 145, 154–172. <https://doi.org/10.1016/j.rse.2014.02.001>
- Ruiz, L. F. C., Guasselli, L. A., Simioni, J. P. D., Belloli, T. F., & Fernandes, P. C. B. (2021). Object-based Classification of Vegetation species in a subtropical wetland using Sentinel-1 and Sentinel-2A images. *Science of Remote Sensing*, 3, 1–10. <https://doi.org/10.1016/j.srs.2021.100017>
- Schmidt, G., Jenkerson, C. B., Masek, J., Vermote, E., & Gao, F. (2013). *Landsat Ecosystem Disturbance Adaptive Processing System (LEDAPS) Algorithm Description* (vi, 9p.). U.S. Geological Survey open-file report, U.S. Geological Survey. <https://doi.org/10.3133/ofr20131057>
- Sowmya, D. R., Deepa, P., & Venugopal, K. (2017). Remote Sensing Satellite Image Processing Techniques for Image Classification: A Comprehensive Survey. *International Journal of Computer Applications*, 161, 24–37. <https://doi.org/10.5120/ijca2017913306>
- Xue, J., & Su, B. (2017). Significant Remote Sensing Vegetation Indices: A Review of Developments and Applications. *Hindawi, Journal of Sensors*, 2017, 1353691. <https://doi.org/10.1155/2017/1353691>
- Yu, M., Xie, Y., & Sha, Z. (2008). Remote sensing imagery in vegetation mapping. *Journal of Plant Ecology*, 1(1), 9–23. <https://doi.org/10.1093/jpe/rtm005>
- Zhu, Z., Fu, Y., Woodcock, C. E., Olofsson, P., Vogelmann, J. E., Holden, C., Wang, M., Dai, S., & Yu, Y. (2016). Including land cover change in analysis of greenness trends using all available Landsat 5, 7, and 8 images: A case study from Guangzhou, China (2000–2014). *Remote Sensing of Environment*, 185, 243–257. <https://doi.org/10.1016/j.rse.2016.03.036>